

The Solar Surface Toroidal Magnetic Field

Roger K. Ulrich and John E. Boyden

*Department of Physics and Astronomy, University of California, Los Angeles, CA
90095-1547*

`ulrich@astro.ucla.edu`

ABSTRACT

The solar cycle of magnetic activity is thought to be a consequence of a dynamo process in which a dipole field produces a toroidal field from differential rotation called the Ω -effect and a twisting process called the α -mechanism that produces a dipole field from the toroidal field. These two magnetic field components are alternately destroyed and recreated in cycle that lasts in total 22 years. Although the dipole field of the sun has long been observed and studied the toroidal field has never before been detected and measured. Our observations provide only line-of-sight components so we use solar rotation to resolve the velocity and magnetic field vectors into a component in the east-west direction and a component in the meridonal-plane. Our analysis of 18.5 years of data using this method reveals for the first time a clear signal of a reversing toroidal magnetic field on the solar surface with strength comparable to that of the well-observed dipole component of the global magnetic field. Our results include meridonal-plane mass flow that shows a zone of convergence near latitudes of 60° implying the subsidence of the toroidally magnetized fluid in this zone. If the toroidal field occupies the bulk of the polar regions of the sun's convective envelope then there is enough magnetic flux to reverse and rebuild the toroidal field at the convective-radiative interface known as the tachocline that is at the inner boundary of the sun's convective envelope. These two steps - the creation of a toroidal field at high latitudes and a mechanism to reverse the tachocline toroidal field - are parts of the dynamo process that have not previously had direct observational support.

Subject headings: sun: magnetic cycle — magnetic dynamo, meridional circulation

1. Introduction

The solar magnetic fields and associated dark sunspots undergo a more or less regular cycle of growth and decay known as the 11-year sunspot cycle. While the detailed physical mechanisms that produce this cycle are incompletely understood, the basic process is believed to come from the interactions between differential rotation, global rotation and the convective motions in the outer solar envelope. As outlined by Babcock (1961), Parker (1955) and Leighton (1969), the greater rotation rate near the solar equator distorts magnetic field lines in a winding-up fashion called the Ω effect. When the toroidal field is adequately strong, it produces paired sunspots by rising to the solar surface in a loop. The Coriolis force on the loop rising in the rotating sun twists the loop in such a way that a new dipole field of the opposite polarity is generated; this is called the α -effect. The operation of both effects produces a repetitive cycle of magnetic field decay and regeneration called an α - Ω dynamo (Krause & Rädler 1980). The dipole field, the differential rotation and the twisting α -effect have all been identified observationally (Babcock & Babcock 1955; Hoeksema 1984; Ulrich et al. 2002) but thus far the toroidal field pattern has not been detected. This letter gives results of an analysis that yields the time and latitude dependence of the sun's surface toroidal field.

2. Analysis Approach

Because our observations only capture the line-of-sight components of the velocity and magnetic field vectors we appeal to solar rotation to reveal the slowly changing part of the vector fields perpendicular to the line of sight. The principle of the method can be illustrated by considering a stationary magnetic field line inclined toward the east relative to the local vertical. As rotation brings this point on the solar surface across the apparent solar disk, the line-of-sight component of the magnetic field will reach a maximum when the point is to the west of the central meridian line. The angular distance from the sun's central meridian to the position of the line-of-sight maximum gives the angular tilt of the vector away from the meridional plane. The first to exploit this approach was Howard (1974) who measured an asymmetry between the magnetic fluxes on the east and west sides of the central meridian line. Howard attributed the measured asymmetry to a general tilt of the magnetic field lines in the direction trailing solar rotation due to the action of the solar wind from a rotating sun. Although a spiral pattern results from this combination of processes in the solar wind, the chromosphere and lower corona are too magnetically rigid to permit the formation of such a spiral in the photosphere (Pneuman & Kopp 1971).

A robust separation of the magnetic and velocity vector fields into slowly varying

longitudinal-plane and east-west components using solar rotation is achieved by tracking points on the surface while they are visible and correlating the line-of-sight projection with both the sine and cosine of the central meridian angle (CMA). This approach was applied by Ulrich (1993) to the velocity field and by Shrauner & Scherrer (1994) to the magnetic field. Ulrich et al. (2002) applied the method to synoptic maps incorporating all available observations of each point during each rotation. The geometry yielding the line-of-sight components of magnetic and velocity vectors is illustrated in figure 1. Based on these geometric considerations, the resolution into the meridonal-plane and east-west direction components is carried out by calculating two weighted averages: the one where the weighting function is $\sin(CMA)$ gives the east- west component and the one where the weighting function is $\cos(CMA)$ gives the meridonal-plane component. The Shrauner-Scherrer approach also includes averages with the product of $\sin(CMA)$ and $\cos(CMA)$ and inverts the 2×2 matrix which results. We find that this approach, while being more accurate is also more sensitive to the coverage of the range of CMA from 90° to $+90^\circ$. Where the coverage of CMA is adequate, we find that resolved components calculated from the full inversion agree well with the values deduced directly from the sine and cosine weighted averages.

As illustrated in figure 1, the direction of the vector velocity or magnetic field on the meridonal plane cannot be determined with our method but can be estimated using other considerations: the large- scale velocity is largely on level surfaces due to mass conservation while the magnetic field is close to vertical except near active regions. We do not apply projection factors to correct for the fact that we see only the line-of-sight component of the meridional velocity on the solar surface. This factor is $\sin(latitude)$. However, in addition to the actual mass motion velocities, the line-of-sight velocity includes the convectively produced limb-effect that comes from correlations between granulation velocities and granulation intensities (Beckers & Nelson 1978). The limb- effect shift is a function of the center-to-limb angle. In order to remove this apparent shift, we subtract from each observed line-of-sight velocity a limb-shift function that is evaluated within a band 13-degrees wide parallel to the solar equator. We choose points in pairs having equal east and west displacements from the central meridian line so that their average is independent of solar rotation. Additionally, we drop from the calculation of the limb shift function all pairs of points for which the magnetic field of either is above 20 gauss to eliminate the influence of magnetically induced line shifts. This selection process yields a function that cannot include any effect of actual material motion along the line of sight. The resulting recession velocity as a function of angular distance from disk center toward the limb is taken as the limb shift function and is subtracted from the recession velocity measured elsewhere on the disk. As long as this velocity vector is parallel to the solar surface, the apparent velocity in the meridonal plane is equal to the actual material velocity times $\sin(latitude)$. We give our results in terms of

this product which we refer to as v_{merid} . Thus, motion toward either pole gives a positive result.

There are a number of small instrumental effects due to errors in the optical configuration of the telescope and spectrograph that influence the meridional velocity determination. In particular, the telescope setting circle used to align the scan direction with the solar equator has its center displaced from the optical axis i.e. the line between the primary objective and the spectrograph entrance slit. Furthermore, we have not corrected for the north-south velocity of the Earth in its orbit projected onto the solar surface. Both these effects have an amplitude that is smaller than but not negligible compared to the measured meridional flow velocities. The net result has been removed using an annual superposed epoch detrending procedure.

3. One-Rotation Average Summary Synoptic Charts

The weighted-average method applied to magnetic and velocity fields yields four products: the east-west velocity field, the meridonal-plane velocity field, the east-west magnetic field and the meridonal-plane magnetic field. For the purpose of studying long-term trends, it is useful to average over a full Carrington rotation so that the spatially-resolved, high amplitude variations are eliminated. The masking effect of these high-amplitude variations otherwise obscures the long-term trends. The earliest time for which the dual averaging methods work successfully is 1986. This is when the Mt. Wilson synoptic program began taking multiple magnetodoppler-grams per day. The resulting synoptic summary charts for the four data products are shown in figure 2. These are given in a sequence of east-west velocity, meridonal-plane velocity, east-west magnetic and meridonal-plane magnetic. Of these the east-west velocity and the meridonal-plane magnetic have been presented numerous times and are referred to as the torsional oscillations (Howard & Labonte 1980; Ulrich 2001; Vorontsov et al. 2002) and the meridonal-plane magnetic field. The deviation of the meridional circulation velocity from a long-term average was included in the figures published by Ulrich (1993). The panel in figure 2 gives the absolute value of the meridional circulation velocity rather than the deviation from the average. Our method of evaluating the limb-shift velocity establishes the velocity at disk center as the zero point of the scale. In this format, this panel represents a new data product. In particular, the time variation in the flow near the pole is remarkable in that it shows a persistent but not-always-present outflow for latitudes above 60° as well as noticeable differences between the north and south hemispheres – the southern hemisphere has a greater circulation rate than the northern hemisphere for cycle 23. The meridional circulation as a function of depth has been studied using helioseismic

ring diagram analysis by Basu & Antia (2003) and Haber et al. (2002). These authors find a significant time dependence to this velocity but give a series of temporally disconnected curves rather than a contour plot. They state that the meridional velocities are low at times of high solar activity in contrast to what is shown in figure 2.

The other new data product is the east-west projection of the magnetic field. This is considered to be positive if the arrow of the field points toward the direction of solar rotation. The average of this field over the full circumference of the small circle at constant latitude must represent a net toroidal field. Thus the plot of east-west magnetic field gives the time and latitude dependence of the sun’s surface toroidal field - clearly a parameter of great interest for the study of the solar dynamo. The presence of a systematic and persistent non-zero result for this toroidal field is significant. We note that Shrauner & Scherrer (1994) did not study this component but rather looked at averages of magnetic field tilt angles. Since these angles are ratios, they do not average linearly and are dominated by those regions where the field strength is small. In order to illustrate the nature of the magnetic field result, we show in figure 3 a short stackplot giving the longitude-resolved line-of-sight field for a single rotation in 1996 averaged over latitudes between 50° N and 60° N. In this plot, time increases downward and only one observation per day is used with the values between observations calculated by interpolation. The scale is between -5 (red) and $+5$ (blue) gauss. The longitudes are calculated relative to an offset point calculated according to the local rotation rate. The positive polarity dominates but there are structures that persist for most of the time they are observable. These may correspond to polar plumes. In addition, there is a pattern where the earliest observations are more negative than the later ones. This corresponds to the magnetic vector pointing against rotation or a negative toroidal field. The toroidal field panel of figure 2 is dominated by negative values for this latitude and time.

4. Discussion

Careful examination of the time and latitude dependence of the four vector projections given in figure 2 reveals a number of interesting properties. Since the figure encompasses nearly a full 22-year cycle, we are able to identify a sequence of events that indicate the mechanism of the magnetic field decline and growth. We start with the time of dipole field reversal when the number of sunspots is near the maximum and describe four steps in the cycle. Following the dipole reversal, the dipole field strength reaches a plateau that persists for about half the 11-year cycle. To make the description definite, consider the north-polar region starting in 1990. This is near the maximum of cycle 22. The northern part of the dipole

field is positive after that year. The magnetic field lines in the bulk of the convective envelope must have a directional sense which points from south to north to maintain continuity of field lines. The faster rotation toward the equator then twists the field lines so that they point against rotation and are negative according to our sign convention. During this time the toroidal field plot shows the development of a weak but pervasive negative component in agreement with the model. This toroidal field is correctly oriented to produce sunspot pairs for the subsequent solar cycle 23 even though cycle 22 is still several years away from its end in 1996. This result is the first time that a critical part of the $\alpha - \Omega$ dynamo - the toroidal field - has been confirmed observationally. It is, however, very weak and in the wrong latitude region to produce the spots and magnetic field of cycle 23.

The second step in the process can now be identified from another of our data products: the meridional circulation. The meridional circulation result for the years 1986 to 1992 was originally presented by Ulrich (1993) in a somewhat different format. We see from this panel of figure 2 that during the years 1986 to 1991 and from 1994 to 1999 there is a zone of convergence near latitude of 60° where the flow from lower latitudes is toward the pole and the flow from higher latitudes is away from the pole. This means that there must be a zone of subsidence in the high latitudes. Dense-pack ring diagram analysis from helioseismic data may have seen an inward extension of this subsidence at latitudes near 50° N from 1999 to 2001 (Haber et al. 2002). As long as the toroidal field pervades the bulk of the convective zone, the total magnetic flux can be much greater than that part which is observed in the solar atmosphere. The bulk inward sweep of the meridional return flow can carry this toroidal field to the inner boundary of the convection zone where it is concentrated into strong flux tubes by the convective motions at this level. Near the maximum of cycle 23, the strength of the toroidal field in the band of solar activity is comparable to that of the meridional plane field that makes up the dipole and active region field. This comparability makes it plausible that both the dipole and toroidal fields are connected as parts of the same process that concentrates and disperses the fields.

After the toroidal field is concentrated at the tachocline, the further development of the dynamo process can follow along the lines discussed by a number of authors (Choudhuri 2003; Gilman 2000; Ossendrijver 2003; Tobias 2002; Rempel et al. 2000; Spruit 2003) the toroidal field is collected into flux tubes where the magnetic buoyancy becomes high enough to permit the magnetized fluid to form a loop that rises through the convective zone to the solar surface to become a sunspot pair. While the loop is moving outward through the rotating solar interior, it experiences a Coriolis force which twists it in the direction to cause the trailing spot to be closer to the pole than the leading spot (Fisher et al. 2000). This trailing spot polarity opposes the existing dipole field and is swept toward the poles by the meridional circulation. Due to the higher average latitude of the trailing spot polarity,

eventually this field component comes to dominate both polar regions and reverses the solar dipole. The cycle can then repeat.

The remaining data product, the torsional oscillation panel of figure 2, is evidently related to the dynamo processes although the nature of this relationship is not readily evident at all stages of the cycle. The plot gives deviations from the average rotation rate that we refer to as speed-up and slow-down. The locations of greatest slow-down correspond to latitudes where the surface toroidal field reverses as is most evident between 1986 and 1989.5 then between 1996 and 2000.5. The locations of greatest speed-up correspond to the latitudes where the toroidal field is strongest although this relationship is less clear. The strength of the torsional pattern is not well correlated with the strength of the magnetic activity. The latitudes of maximum speed-up and slow-down are well defined through the minima of 1986 and 1996 where the meridonal-plane magnetic fields are largely absent. Furthermore, the torsional oscillation plot includes a strong difference between the northern and southern hemispheres. The south has a strong excess of rotation speed-up compared to the north where there is near equality between times of speed-up and slow-down. While there are some north-south asymmetries in the meridonal-plane magnetic field, these are not nearly as strong as are seen in the torsional oscillation case.

5. Conclusions

The clues we have found as to the sequence of phenomena may be helpful to the continued development of dynamo models. In particular the fact that the toroidal field permeates the convective envelope out to the solar surface rather than being confined to the tachocline layer means that there is a larger volume to provide the magnetic flux. The presence of the subsidence zone makes it possible to transport this flux to the zone where it can be effectively amplified and reconfigured into intense flux tubes that ultimately become sunspots. We have identified two puzzling aspects of the process that deserve further study, namely: the polar outflow component of the meridional flow and the close coupling between the torsional oscillations and the toroidal field.

Another point concerning the meridional flow velocity is our lack of an explanation for the polar outflow during much of the period covered by our data. This is not a part of most meridional circulation models but is important for our model of subsidence in the high latitudes. The strength of the polar outflow seems to be reduced around the time of dipole reversal.

The toroidal field measurement presented in figure 2 would not provide evidence of

a solar effect if it were restricted to a period of time less than a major fraction of the full 22-year Hale cycle. The weak polar components might easily be explained away as an instrumental effect. However, the close correspondence with other features of the solar cycle and the fact that the weak fields reverse following the dipole field reversal makes appeal to spurious instrumental effects an unlikely explanation for the results. We are unaware of any instrumental effect that could give rise to the time and latitude dependent pattern we see in figure 2.

We wish to thank Jack Harvey, Peter Gilman, Luca Bertello and Ferenc Varadi for their helpful comments on a draft of this letter. Due to the extended nature of the time base used in this work no single grant or agency can be cited as supporting this work. The support has come from NASA’s Solar Physics and Living with a Star programs, from NSF’s Solar-Terrestrial office and the Navy’s Office of Scientific Research.

REFERENCES

- Babcock, H. W. 1961, *ApJ*, 133, 572
- Babcock, H. W. & Babcock, H. D. 1955, *ApJ*, 121, 349
- Basu, S. & Antia, H. M. 2003, *ApJ*, 585, 553
- Beckers, J. M. & Nelson, G. D. 1978, *Sol. Phys.*, 58, 243
- Choudhuri, A. R. 2003, *Sol. Phys.*, 215, 31
- Fisher, G. H., Fan, Y., Longcope, D. W., Linton, M. G., & Pevtsov, A. A. 2000, *Sol. Phys.*, 192, 119
- Gilman, P. A. 2000, *Sol. Phys.*, 192, 27
- Haber, D. A., Hindman, B. W., Toomre, J., Bogart, R. S., Larsen, R. M., & Hill, F. 2002, *ApJ*, 570, 855
- Hoeksema, J. T. 1984, Ph.D. Thesis
- Howard, R. 1974, *Sol. Phys.*, 39, 275
- Howard, R. & Labonte, B. J. 1980, *ApJ*, 239, L33

- Krause, F. & Rädler, K. H. 1980, Mean-field magnetohydrodynamics and dynamo theory (Oxford: Pergamon Press, 1980)
- Leighton, R. B. 1969, *ApJ*, 156, 1
- Ossendrijver, M. 2003, *A&A Rev.*, 11, 287
- Parker, E. N. 1955, *ApJ*, 121, 491
- Pneuman, G. W. & Kopp, R. A. 1971, *Sol. Phys.*, 18, 258
- Rempel, M., Schüssler, M., & Tóth, G. 2000, *A&A*, 363, 789
- Shrauner, J. A. & Scherrer, P. H. 1994, *Sol. Phys.*, 153, 131
- Spruit, H. C. 2003, *Sol. Phys.*, 213, 1
- Tobias, S. M. 2002, *Royal Society of London Philosophical Transactions Series A*, 360, 2741
- Ulrich, R. K. 1993, in *ASP Conf. Ser. 40: IAU Colloq. 137: Inside the Stars*, 25–42
- Ulrich, R. K. 2001, *ApJ*, 560, 466
- Ulrich, R. K., Evans, S., Boyden, J. E., & Webster, L. 2002, *ApJS*, 139, 259
- Vorontsov, S. V., Christensen-Dalsgaard, J., Schou, J., Strakhov, V. N., & Thompson, M. J. 2002, *Science*, 296, 101

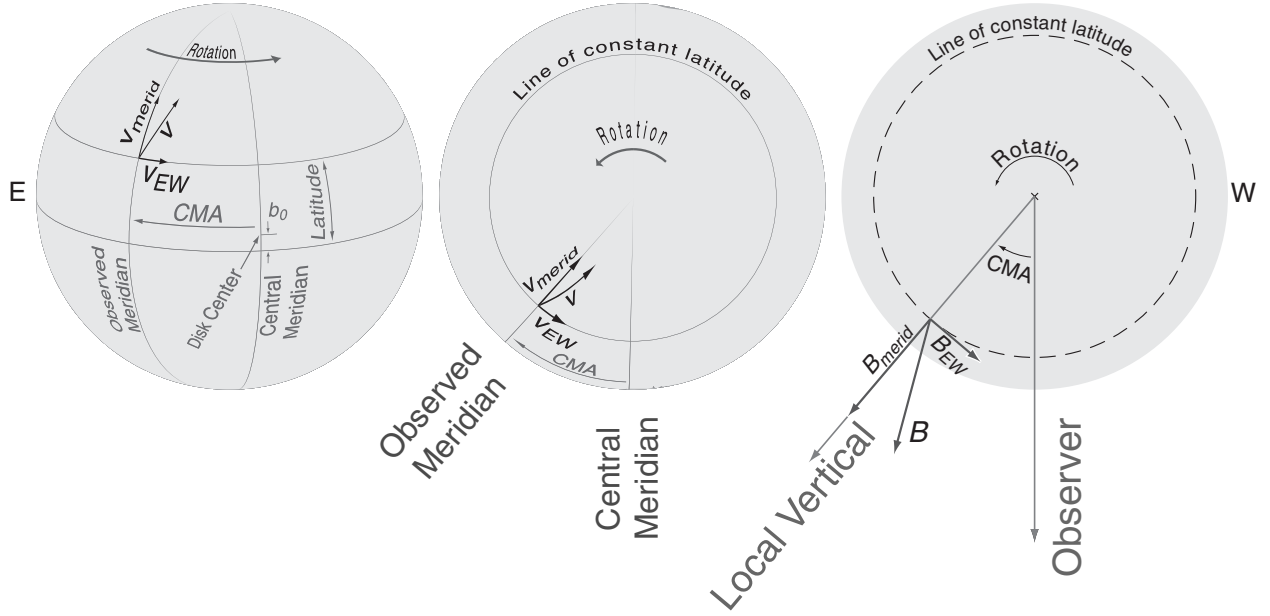


Fig. 1.— Illustration of the 3-dimensional geometry used to resolve the meridional and EW components of the magnetic field and velocity field. The velocity vector v is along the solar surface and the geometry of its two components is shown in the left and center figures. We determine two components: v_{merid} and v_{EW} that are the meridional and east-west (zonal) velocities. The line-of-sight projection of v_{merid} includes a factor of $\sin(\text{latitude})$ and is positive for motions toward the poles in both northern and southern hemispheres. The right figure shows a pole-eye view of a magnetic field vector which includes components in the meridional plane and a component in the east-west (zonal) direction. The line-of-sight component of the magnetic field is the sum of the projection of these two components or $B_\ell = B_{merid} \cos(CMA) + B_{EW} \sin(CMA)$ where B_{merid} is the projection of the magnetic field onto the line which is the intersection of the meridional plane and the east-west plane. Note that the sign convention is such that a vector pointing in the direction of rotation has positive $E - W$ component. A 3-dimensional rendering of this geometry is in Ulrich et al. (2002).

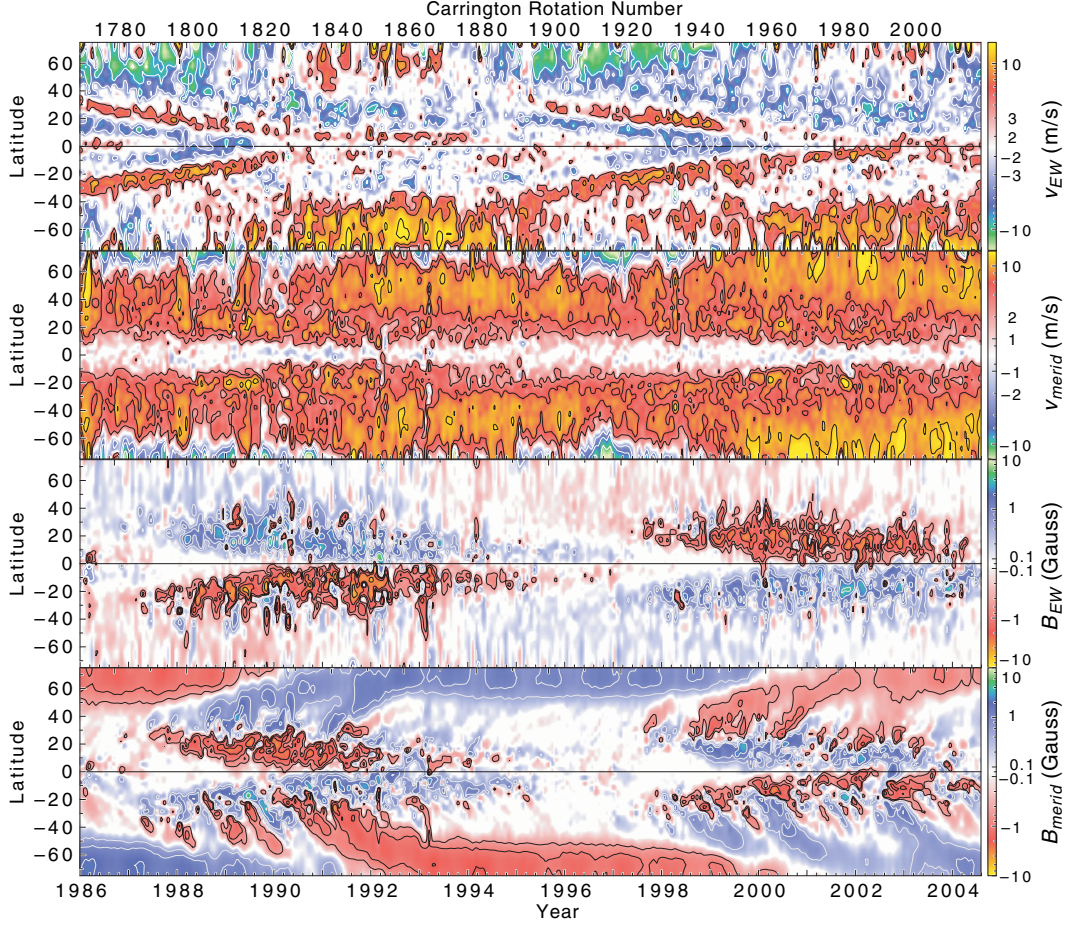


Fig. 2.— Summary averages of magnetic and velocity measurements from the Mt. Wilson synoptic program carried out at the 150-solar tower telescope. The vector fields have been resolved into east-west and rotation-plane components by carrying out sine and cosine weighted averages for each point over the period time it is on the Earth-facing side of the sun each rotation. These panels give a secondary average of the longitude-dependent, weighted averages over all Carrington longitudes for each Carrington rotation. The resolved components are given in the sequence: east-west velocity, meridonal-plane velocity, east-west magnetic and meridonal-plane magnetic. The symbolic representations we use for each of these quantities are to the right of the color-bar giving the scale for each panel. The contour levels are at ± 16 , ± 8 and ± 4 m/s for the torsional oscillation panel, ± 12 , ± 6 and ± 3 m/s for the meridional circulation panel and at ± 4 , ± 2 , ± 1 and ± 0.5 gauss for both magnetic field panels.

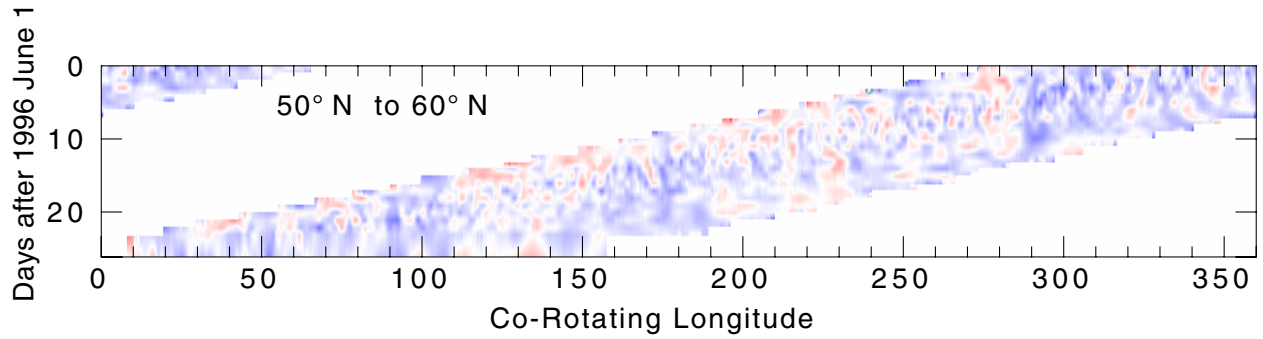


Fig. 3.— A stackplot segment for a polar region near solar minimum. The period is 1996 June 1 to 1996 June 27 and the latitude band is from 50° N to 60° N. The field strength shown is for the raw line-of-sight component. The observations used are restricted to the higher spatial resolution, slow-scan program with an entrance aperture of $12''$ on a side. This entire band would be averaged together to form a single point in figure 2.